

SLAC-PUB-3225

October 1983

T/E

PRODUCTION OF SCALAR LEPTONS IN W AND Z BOSON DECAY*

R. MICHAEL BARNETT

Institute for Theoretical Physics

University of California, Santa Barbara, California 93106

HOWARD E. HABER

Department of Physics, University of California

*Santa Cruz, California 95064***

and

Stanford Linear Accelerator Center

Stanford University, Stanford, California 94305

KLAUS S. LACKNER***

Stanford Linear Accelerator Center

Stanford University, Stanford, California 94305

Submitted to Physical Review D

*Work supported in part by the Department of Energy contract number DE-AC03-76SF00515.

** Permanent address.

*** Address as of October 4, 1983: Los Alamos National Laboratory, Los Alamos, New Mexico 87545.

ABSTRACT

Alternative decay modes of the W and Z bosons may provide a method either to discover the supersymmetric partners of leptons or to set greatly improved limits on their masses. Details are provided on these methods, and various distributions are shown for separating potential backgrounds. If $\bar{p}p \rightarrow W \rightarrow e_s \nu_s$ is allowed, a clear signal for supersymmetry could be established from future data. In e^+e^- annihilation a distinctive signature for scalar neutrinos could be jets plus an electron all confined to a single hemisphere (with substantial missing energy). Even more dramatic but rarer would be events with only $e^+ + \mu^-$ together in one hemisphere and all other energy missing.

1. Introduction

Theories of supersymmetry¹ predict a partner for each presently known particle, but no evidence has yet been found in nature for such particles.² Although there are aesthetic and practical motivations for maintaining our interest in supersymmetry,³ any experimental evidence would give us critical guidance in developing a realistic theory. The production of W and Z bosons at the CERN SPS collider⁴ will soon provide us with an excellent opportunity to search for supersymmetry via non-standard decay modes of these bosons.

Experiment tells us that the supersymmetric partners of the ordinary fermions must be quite heavy.⁵ In most cases, the lower limits on their masses have been set in the range 19-24 GeV. Furthermore, in almost all models,⁶ supersymmetric particles carry a negative R -parity⁷ (as compared to a positive R -parity for the ordinary particles). This means that new supersymmetric particles must be produced in pairs. Second, even though certain models predict a light supersymmetric particle, the photino, it can be produced only by the exchange of a heavy supersymmetric scalar. Thus, production rates of new light supersymmetric particles will be small (e.g. of weak interaction size if the scalar particles are equal in mass to the W -boson).⁸ Therefore supersymmetric particle production is likely to be quite rare at present energies. It is therefore not appropriate to look for subtle effects which can be confused with other particles or with some ordinary higher-order corrections. We believe that the best way to look for supersymmetry is to look for processes with very distinctive signatures for which backgrounds are either small or nonexistent. We will show that scalar lepton production in $p\bar{p}$ colliders and in e^+e^- annihilation offers just such an opportunity.

As we perform calculations of various supersymmetric processes, we shall

strive to minimize the model dependence of the predictions. Otherwise, calculations would be problematical since there is as yet no truly compelling model of supersymmetry. We choose to use a simple, softly broken supersymmetric model of electroweak interactions which is described in detail in ref 9. In its simplest form, supersymmetry breaking is imposed via explicit mass terms for scalar quarks and leptons. This approach is motivated in part by recent work in supergravity which shows that the effective low-energy theory of a spontaneously broken supergravity coupled to matter fields is a globally supersymmetric theory broken by various soft terms.¹⁰⁻¹²

Recently, there has been a large amount of work discussing ways in which supersymmetry could be discovered by present and future experiments.¹³ In particular much interest has been focused on the decays of W and Z bosons into supersymmetric particles. In this paper, we shall elaborate on results concerning the production of scalar leptons, first presented by us in ref. 14. Studies on W and Z decays into supersymmetric scalars have also been carried out in refs. 15-17. In addition, one can also study W and Z decays into supersymmetric fermions¹⁷⁻¹⁹ (partners of the gauge and Higgs bosons). These events are expected to be equally distinctive and have been studied in detail in ref. 19. It is interesting to note that both classes of events often display similar signatures. If such signatures are eventually observed, careful analysis will be needed to distinguish among various "non-standard physics" interpretations. The production and decay of W bosons in the $p\bar{p}$ collider is likely to provide a sensitive test of the existence or non-existence new phenomena. The Z^0 is produced less copiously there, and one will probably have to wait for the Z^0 factories (e^+e^- machines)

at SLC or LEP. The e^+e^- machines also provide us with the possibility of observing continuum annihilation of e^+e^- into a pair of supersymmetric scalars or fermions. The latter point has been discussed extensively in ref. 20.

In Section 2 we discuss the production of scalar leptons at the CERN SPS collider which could occur via the decays of the W boson. (Some useful computations are provided in an appendix.) We also study in detail the potential backgrounds. In Section 3 we describe dramatic signals which could appear in Z^0 decay into a pair of supersymmetric scalar neutrinos. Although this is in principle observable at the CERN $p\bar{p}$ collider, one will have to wait for the Z^0 factories (e^+e^- machines SLC and LEP which will run at the Z^0 resonances) in order to be really sensitive to supersymmetric decays of the Z^0 . In addition it may be possible to obtain limits on scalar neutrino masses by searching for $e^+e^- \rightarrow \nu_s \bar{\nu}_s$ at lower energies below the Z^0 . Finally, the production of charged scalar lepton pairs is briefly mentioned. We state our conclusions in Section 4.

2. Production of Supersymmetric Particles in W Decay

The $e_s \nu_s$ decay mode²¹ of the W boson produced in $p\bar{p}$ scattering could offer a very distinctive signature for supersymmetry. This would be especially true if the ν_s decays invisibly (the expected decay of e_s is to $e + \tilde{\gamma}$). For convenience we always refer to $e_s \nu_{e_s}$, but we of course wish to include $\mu_s \nu_{\mu_s}$ and $\tau_s \nu_{\tau_s}$. There are now more than 80 events in $p\bar{p} \rightarrow W + \text{anything}$ with $W \rightarrow e\nu$ which have been observed at the CERN SPS collider.⁴ Many more W boson events are expected after running resumes, so that it will be feasible to search for alternative decay modes of the W . The $e_s \nu_s$ mode could be substantial if the masses of e_s and ν_s are not too large. The ratio of the $e_s \nu_s$ mode to the $e\nu$ mode is

$$r \equiv \frac{\Gamma(W^+ \rightarrow e_s^+ \nu_s)}{\Gamma(W^+ \rightarrow e^+ \nu)} = \frac{1}{2} \left[\left(1 - \frac{M_{\nu_s}^2}{M_W^2} - \frac{M_{e_s}^2}{M_W^2} \right)^2 - 4 \frac{M_{\nu_s}^2 M_{e_s}^2}{M_W^4} \right]^{\frac{3}{2}} \quad (1)$$

For example, from eq. 1 or from fig. 1 we see that for $M_{\nu_s} = M_{e_s} = 30 \text{ GeV}$, we have $r = 0.16$ while for $M_{\nu_s} = M_{e_s} = 20 \text{ GeV}$, we have $r = 0.33$.

Although several $W \rightarrow e_s \nu_s$ events may already have been produced at the SPS collider, the identification of such events requires their separation from backgrounds. Backgrounds include $W \rightarrow e\nu$, $W \rightarrow \nu\tau$ ($\tau \rightarrow e\nu D$), and the semileptonic decays of a pair of heavy quarks. The $e_s \nu_s$ events superficially resemble $e\nu$ events since e_s decays into $e + \tilde{\gamma}$, and the photino $\tilde{\gamma}$ and the ν_s decay products (by assumption) leave the detector unobserved. However, their separation from backgrounds will not be as easy as it was for $W \rightarrow e\nu$ primarily because the $e_s \nu_s$ mode could be confused with the larger $e\nu$ mode, and because for the $e_s \nu_s$ events the p_e^\perp spectrum does not peak at such high momenta.

To aid in the identification of $\nu_s e_s$ events, we have calculated a variety of distributions of νe , $\nu\tau$ and $\nu_s e_s$ processes (under the assumption that ν_s decays

invisibly). We used Monte Carlo techniques to simulate W bosons with the appropriate longitudinal and transverse momentum distributions.

For the transverse momentum distributions we followed Halzen, Martin and Scott²² whose results can be approximately parameterized at $Q^2 = M_W^2$ as

$$\frac{d\sigma}{dp_{\perp}^2} \propto 6 e^{-p_{\perp}/3.5} + e^{-p_{\perp}/10}. \quad (2)$$

Making large changes in this distribution (such as dropping the second term in eq. 2) has very little impact on our results.

For the longitudinal distributions we use Drell-Yan techniques²³ and the Owens-Reya parameterization²⁴ of the u and d quark distributions. Again our results are not sensitive to changes in this distribution. Using the same techniques, the simulated W bosons were allowed to decay into $e\nu$, $\pi\nu$, or $e_s\nu_s$. The scalar electrons e_s (or τ) were then allowed to decay into $e\tilde{\gamma}$ (or $e\nu D$). Using the standard model of electroweak interactions, the $e\nu$ (and $\pi\nu$) decay modes were given a $(1 \pm \cos \theta)^2$ dependence and the $e_s\nu_s$ decay modes a $\sin^2 \theta$ dependence in the center of mass.

To simulate experimental conditions, we then assumed that one can observe only five variables: the electron's longitudinal momentum and the two components of the transverse momenta of the electron and of the W boson (the latter measured from the hadronic transverse momentum $\vec{p}_{\text{had}}^{\perp}$). We have defined five variables (for plotting) which are defined in the context of $W \rightarrow e\nu$: the absolute transverse momenta of the electron and the neutrino, $\cos \theta$ (where $\theta =$ angle between electron and proton beam), the longitudinal momentum of the neutrino

and the transverse mass. Where the neutrino enters, our definitions are:

$$\vec{p}_\nu^\perp \equiv -\vec{p}_{had}^\perp - \vec{p}_e^\perp \quad (3)$$

$$p_{\nu(\pm)}^\parallel \equiv \frac{m_W^2 + 2\vec{p}_\nu^\perp \cdot \vec{p}_e^\perp}{2p_e^{\perp 2}} \left\{ p_e^\parallel \pm p_e \sqrt{1 - \frac{4p_\nu^{\perp 2} p_e^{\perp 2}}{(M_W^2 + 2\vec{p}_\nu^\perp \cdot \vec{p}_e^\perp)^2}} \right\} \quad (4)$$

$$m_T \equiv \vec{p}_e^\perp \cdot \vec{p}_\nu^\perp . \quad (5)$$

The ambiguity in eq. 5 for p_ν^\parallel is often unresolvable. We therefore define a variable p_m in terms of the minimum of the absolute value of the two solutions for p_ν^\parallel :

$$p_m \equiv \text{sign}(p_\nu^\parallel) \cdot \text{Min} |p_{\nu(\pm)}^\parallel| . \quad (6)$$

Clearly, some of these variables lose their simple kinematical significance when we consider $W \rightarrow \tau\nu$ and $W \rightarrow e_s\nu_s$. Nonetheless they remain both well defined and quite useful.

Let us first consider the distributions for $W \rightarrow e\nu$ and $W \rightarrow e_s\nu_s$ derived as described above. The transverse momentum spectra of the electrons for several choices of M_{e_s} and M_{ν_s} are shown in fig. 2(a). If a much sharper p_\perp spectra is assumed for the W bosons (as described above), then the tails of the spectra above $p_\perp = 45$ GeV disappear while other aspects are unchanged. In all other figures we have excluded events with

$$p_e^\perp < 12 \text{ GeV} . \quad (7)$$

The actual choice for this cut must be made based on experimental considerations such as the need to eliminate background.

Momentum conservation assures that the $p_{\bar{\nu}}^{\perp}$ distribution shown in fig. 2(b) looks roughly similar to the p_e^{\perp} distribution. Recall that for $W \rightarrow e_s \nu_s$, $p_{\bar{\nu}}^{\perp}$ does not have the physical significance as it does for $W \rightarrow e\nu$. It is clear that the average values of both $p_{\bar{\nu}}^{\perp}$ and p_e^{\perp} are large for $W \rightarrow e_s \nu_s$ events, but as expected they are significantly smaller than for $W \rightarrow e\nu$ events.

For $e^- \bar{\nu}$ events, the $\cos \theta$ distribution in the lab frame (fig. 2(c)) reflects the $(1 + \cos \theta)^2$ dependence for $\bar{u} d \rightarrow W^- \rightarrow e^- \bar{\nu}$ which would occur if W were at rest. The forward-backward asymmetry is still clearly evident, even though the distribution has been modified somewhat. However, for $e_s \nu_s$ events the $\cos \theta$ distribution is quite different from that for $e\nu$ events. The center-of-mass $\sin^2 \theta$ distribution is modified to a relatively flat distribution.

The distributions of p_m shown in fig. 2(d) look quite different for $e\nu$ and $e_s \nu_s$ events. The dip which occurs for $e_s \nu_s$ events is difficult to interpret since this variable has no simple physical significance here though it is well-defined. For completeness we show the distribution of transverse mass (fig. 2(e)) although we make no use of it. These figures do not account for experimental resolution or efficiencies.

Since we expect $e\nu$ events to outnumber $e_s \nu_s$ events (by 6 to 1 if $M_{e_s} = M_{\nu_s} = 30 \text{ GeV}$), we have used fig. 2 to suggest cuts which will greatly reduce the number of $e\nu$ events relative to $e_s \nu_s$ events. In particular we have chosen to eliminate all events with $p_e^{\perp} > 33 \text{ GeV}$, or $p_{\bar{\nu}}^{\perp} > 35 \text{ GeV}$, or $\cos \theta > 0.7$ or $-40 < p_m < 20 \text{ GeV}$ (these cuts are slightly different from those in ref 14). We find that these cuts eliminate 90% of $e\nu$ events but only a third of the $e_s \nu_s$ events. For $M_{e_s} = M_{\nu_s} = 30 \text{ GeV}$ this means that approximately equal numbers of $e\nu$ and $e_s \nu_s$ events survive. These cuts are, of course, not uncorrelated (often

they eliminate the same events).

What remains after the cuts are made is shown in fig. 3. Although the overall scale is arbitrary, the relative renormalization of these curves is fixed. Distributions such as fig. 3(a),(c), and (d) would be particularly useful then in demonstrating the presence of a signal for supersymmetry. There still remain other backgrounds. If $W \rightarrow \nu\tau$ and $\tau \rightarrow e\nu\nu$, one obtains a similar signal. However, once we know the $W \rightarrow e\nu$ rate, this rate is precisely calculable (see appendix), and this background can be subtracted. The distributions are also calculated and are shown in fig. 4. As expected, the p_e^\perp distribution is softer, and there is a forward-backward asymmetry (though not as pronounced, as for $W \rightarrow e\nu$ events). In summary, this background is comparable in rate to the signal ($e_s\nu_s$), but can be subtracted.

Another source of background is the production of a pair of heavy quarks both of which decay semileptonically. A small fraction of such events will have the energy of one quark's decay go primarily into an electron while the energy of the other quark's decay goes primarily into a neutrino. Monte Carlo studies done elsewhere suggest that this background is not a problem.²⁵ However, one can actually measure this background to a fair approximation by looking for $e\mu$ (and $e^\pm e^\pm$) events where the events have characteristics similar to those of fig. 2 (in particular, there are large transverse masses, large perpendicular momenta and little transverse hadronic energy). We believe there is no evidence for such events.

To use this technique to find evidence for supersymmetric particles in the region $r \approx 1/6$ (for example, $M_{\nu_s} \approx M_{e_s} \approx 30$ GeV or $M_{e_s} \approx 40$ GeV, $M_{\nu_s} \approx 10$ GeV), one will need more events than are currently available. When 300

events with $W \rightarrow e\nu$ are obtained (so that we may hope to have 40-60 events with $W \rightarrow e_s\nu_s$), then it may be possible to find supersymmetric particles or to set limits on their masses.

If there is a signal for new physics, one then must ask whether this signal necessarily indicates supersymmetry. There may be a new heavy lepton²⁶ ($W \rightarrow \nu L$) which will decay occasionally into $\nu\nu e$. There may be other supersymmetric processes which could imitate the $W \rightarrow e_s\nu_s$ mode. For example, one could have $W \rightarrow \tilde{\gamma}\omega$ ($\omega \equiv$ wino), and occasionally then $\omega \rightarrow e\nu_s$.¹⁷⁻¹⁹ These processes would of themselves be very interesting and would require further consideration. We are at present investigating some of these possibilities.²⁷ One additional consequence of the existence of new decay modes is that the branching ratios for the standard modes (e.g. $BR(W \rightarrow e\nu) \approx 8\%$) would be reduced. In summary the ability to produce large number of W bosons gives us a new window into supersymmetry.

3. Production of Scalar Leptons in Z^0 Decay and e^+e^- Physics

Supersymmetric leptons can also be produced by Z^0 decays. The frequency of such decays can be obtained from:

$$\frac{\Gamma(Z^0 \rightarrow \ell_s \ell_s)}{\Gamma(Z^0 \rightarrow \ell \ell)} = \frac{1}{2} \left(1 - \frac{4M_{\ell_s}^2}{m_Z^2}\right)^{3/2} \quad (8)$$

where ℓ_s can be a charged scalar lepton or a scalar neutrino (and the mass of the lepton ℓ has been neglected). But, the Z^0 is produced far less copiously than the W at the CERN SPS collider. Therefore, it may be only the Z^0 factories (e^+e^- machines SLC and LEP) which will be able to make definitive statements regarding possible supersymmetric decay modes of the Z^0 . However, it is worth considering briefly what these scalar leptonic decays of the Z^0 would look like at the $p\bar{p}$ collider.

First, consider $p\bar{p} \rightarrow Z^0 + X$, $Z^0 \rightarrow e_s^+ e_s^-$ which was analyzed by Cabibbo et al. in ref. 16. They argue that such events would *a priori* be swamped by Drell-Yan events since $e_s^\pm \rightarrow e^\pm + \tilde{\gamma}$ with the photino escaping leads to the appearance of e^+e^- pairs at invariant mass substantially below m_Z . One can in principle make use of the missing (photino) transverse energy signal to eliminate most Drell-Yan events. As we found in W -decay, one still must contend with backgrounds which in this case include $\tau^+\tau^-$ -Drell-Yan and double semi-leptonic decay of heavy quarks which can also result in substantial missing energy. Cabibbo et al. estimate that a high luminosity run at the CERN collider over the next few years might be sensitive to scalar electron masses up to 40 GeV.

Second, consider $p\bar{p} \rightarrow Z^0 + X$, $Z^0 \rightarrow \nu_s \bar{\nu}_s$. If the scalar neutrino decays invisibly (as assumed in the previous section), then these events will be unobservable. However, we have argued in ref. 28 that for certain sets of parameters, a

significant fraction of the ν_s will decay into charged modes such as $\nu_s \rightarrow e^- u \bar{d} \tilde{g}$, $\nu_s \rightarrow \nu u \tilde{u} \tilde{g}$ (where \tilde{g} is the gluino) or if kinematically allowed, $\nu_s \rightarrow e_s u \bar{d}$.⁹ These results have been summarized in fig. 5. Of particular interest are events where one of the scalar neutrinos decays into charged particles and the other decays invisibly. This could lead to events with a hadronic jet with *no* visible charged lepton and a lot of missing transverse momentum (due to an escaping ν_s). It is possible that such events could be observed at the CERN collider, but it requires a substantial number of Z^0 events and a favorable choice of parameters in the supersymmetric model which could lead to interesting signatures.

In summary, it is not inconceivable that scalar leptonic decay modes of the Z^0 could be observed at the CERN $p\bar{p}$ collider. However, many years of running will be required to obtain a large enough sample of Z^0 events by which time the Z^0 factories SLC and LEP will be turning on. We therefore turn to an analysis of scalar lepton production in e^+e^- annihilation both on and off the Z^0 resonance.

In searching for supersymmetry, the potential backgrounds are much smaller in e^+e^- physics than in $p\bar{p}$ physics. Just a few events can lead to a very clear signal. On the other hand present-day e^+e^- machines do not reach the energies currently available at $p\bar{p}$ colliders. Therefore, much of our discussion is concentrated on future experiments at TRISTAN, SLC, and LEP. First, let us briefly consider the production of pairs of charged scalar leptons. This has been discussed in detail in the literature¹³ so we simply summarize the main points here. Corresponding to each charged lepton, there are two charged scalar leptons.²¹ Because they are scalar particles, they are produced in e^+e^- annihilation with an asymptotic cross section equal to 1/4 unit of R (where one unit of $R = \sigma(e^+e^- \rightarrow \gamma \rightarrow \mu^+\mu^-)$), with angular distribution $\sin^2\theta$. The scalar leptons

decay via $\ell_s \rightarrow \ell + \tilde{\gamma}$ and we shall assume that the photino is light and escapes undetected.²⁹ Experimentally, $e^+e^- \rightarrow \ell_s \bar{\ell}_s$ would resemble the production of a new heavy lepton (because of the missing photino energy). Two major differences would be the $\sin^2 \theta$ distribution in the production and the P -wave suppression factor near threshold. Discussions of experimental techniques for scalar lepton searches can be found in ref. 5.

In the remainder of this section, we will focus on the pair production of scalar neutrinos in e^+e^- annihilation. This process may occur with a clear signature below the threshold for the pair production of scalar electrons. Therefore, it is already interesting to consider $\nu_s \bar{\nu}_s$ production at energies currently available. However, this process becomes particularly interesting, as the available energy approaches the mass of the Z^0 . As we will point out, running on the Z^0 resonance will lead to cross sections large enough to look for very rare decay modes which allow a remarkably clean identification of the processes involved. Furthermore, these processes can be chosen in such a way as to minimize the number of model-dependent assumptions.

The process $e^+e^- \rightarrow \nu_s \bar{\nu}_s$ occurs via s-channel Z^0 and t-channel wino exchange. If ν_s has only invisible decays, (e. g. $\nu_s \rightarrow \nu \tilde{\gamma}$), then the only way to observe production of ν_s is to rely on neutrino-counting techniques³⁰; i.e. $e^+e^- \rightarrow \gamma + \text{missing neutrals}$. There are, however, charged-decay modes of the scalar neutrino which are significant, if M_{q_s} and M_{e_s} are not more than some 30% above M_{ν_s} , as shown in fig. 5. Under those conditions, the dominant charged decays are the hadronic decays which include final state gluinos.³¹ These charged decays of the scalar neutrino can lead to very distinctive signatures in e^+e^- physics. When one ν_s decays invisibly while the other ν_s decays into charged

modes such as $e^- u \bar{d} \tilde{g}$ or $\nu u \bar{u} \tilde{g}$, one obtains a highly unbalanced event where more than half the energy is missing. Computer simulated examples of such events are shown in figs. 6 and 7. Typically, one hemisphere is empty, and the total visible momentum has a large component perpendicular to the beam. One has to keep in mind that the outgoing quarks and gluinos will fragment into jets. The available energy is normally large enough to form relatively narrow jets, and they will be pointing into one hemisphere.

If the gluino were not light, these remarks would have to be modified. The “gluino jet” would be substantially broadened. Its decay ($\tilde{g} \rightarrow q \bar{q} \tilde{\gamma}$) would sometimes result in particles in the other hemisphere which would make this signature somewhat less distinctive.

The differential cross section for $e^+ e^- \rightarrow \nu_s \bar{\nu}_s$ (neglecting the electron mass) at a center-of-mass energy \sqrt{s} is given by

$$\begin{aligned} \frac{d\sigma}{d\cos\theta} = & \frac{\pi\alpha^2 s}{32X^2} \left(1 - \frac{4M^2}{s}\right)^{3/2} \sin^2\theta \\ & \times \left\{ \frac{1}{(m_\omega^2 - t)^2} + \left(\frac{(4X-1)^2 + 1}{8(1-X)^2}\right) \left(\frac{1}{(m_Z^2 - s)^2 + \Gamma^2 m_Z^2}\right) \right. \\ & \left. + \left(\frac{2X-1}{1-X}\right) \left(\frac{1}{m_\omega^2 - t}\right) \left(\frac{M_Z - s}{(m_Z - s)^2 + \Gamma^2 m_Z^2}\right) \right\} \end{aligned} \quad (9)$$

where $X \equiv \sin^2\theta_W$, $M \equiv M_{\nu_s}$, and $t = M^2 - \frac{s}{2} + \frac{s}{2} \left(1 - \frac{4M^2}{s}\right)^{1/2} \cos\theta$. The threshold behavior and the overall $\sin^2\theta$ dependence reflect the p -wave nature of this process and result from the spin of ν_s and its chiral couplings. This can be integrated over $\cos\theta$ to obtain the total rate for $\nu_s \bar{\nu}_s$ production. We will normalize the total cross section in units of R . We then find that

$$R(\nu_s \bar{\nu}_s) = \frac{3}{16X^2} (R_1 + R_2 + R_{12}), \quad (10a)$$

$$R_1 = -2 \left(1 - \frac{4M^2}{s} \right)^{1/2} + \left(\frac{s - 2M^2 + 2m_W^2}{s} \right) \log \left(\frac{m_W^2 - t_-}{m_W^2 - t_+} \right) \quad (10b)$$

$$R_2 = \frac{[(4X - 1)^2 + 1]}{48(1 - X)^2} \left(1 - \frac{4M^2}{s} \right)^{3/2} \frac{s^2}{(m_Z^2 - s)^2 + \Gamma^2 m_Z^2} \quad (10c)$$

$$R_{12} = \frac{2X - 1}{1 - X} \frac{(m_Z^2 - s)}{(m_Z^2 - s)^2 + \Gamma^2 m_Z^2} \times \left[\left(1 - \frac{4M^2}{s} \right)^{1/2} \left(\frac{1}{2} s + m_W^2 - M^2 \right) - \frac{(m_W^2 - M^2)^2 + m_W^2 s}{s} \log \left(\frac{m_W^2 - t_-}{m_W^2 - t_+} \right) \right] \quad (10d)$$

where $t_{\pm} = t(\cos \theta = \pm 1)$. Although it is not obvious upon inspection, note that $R(\nu_s \bar{\nu}_s)$ is proportional to $\left(1 - \frac{4M^2}{s} \right)^{3/2}$ in the limit where $s \rightarrow 4M^2$. A plot of $R(\nu_s \bar{\nu}_s)$ for various energies of interest is presented in fig. 8. We have assumed $M_{wino} = m_W$.³² If the wino is significantly lighter than the W , these rates may be significantly enhanced. Here the wino has been defined as the appropriate mixture of the charged gaugino and higgsino as determined by the mass matrix.¹⁷⁻¹⁹ The rates we refer to are enhanced only if the light wino consists dominantly of gaugino components (since the Higgsino couplings are proportional to fermion masses). This is a model-dependent question.³³ However, the rates are unlikely to be much less than those given in eq. 10 unless both wino masses are substantially heavier than the W mass.

Taking into account the pair production of $\nu_{e\mu}$, $\nu_{\mu s}$ and $\nu_{\tau s}$, one can estimate (using eq. 10) the number of events to be expected at different e^+e^- machines. At PETRA for a luminosity of $1.3 \times 10^{31} \text{ sec}^{-1} \text{ cm}^{-2}$ at $\sqrt{s} = 42 \text{ GeV}$, and $M_{\nu_s} = 18 \text{ GeV}$ a year's running (with 50% uptime) may yield 14 events with one neutral and one charged decay. At TRISTAN ($\sqrt{s} = 60 \text{ GeV}$) assuming the

same luminosity and the same mass for the scalar neutrinos, a year's running may yield 450 such events. This last number seems to be sufficient to detect a scalar neutrino due to its hadronic decay under a wide range of mass parameters. In any case it will be possible to put more stringent constraints on the scalar lepton masses. However, for these hadronic decays the constraints will depend on the masses assumed for the supersymmetric partners of the quarks (and the gluino mass).

At SLC and LEP one will run directly on the Z^0 resonance. This will either result in a large production cross section for scalar neutrinos or set very high limits on the masses. Because of the high production cross section, one is not restricted anymore to the hadronic decays of the scalar neutrino. Instead it becomes possible to study the rare leptonic decay channels which show even more dramatic decay signatures. Furthermore, these decay channels have the added advantage of being less dependent on model assumptions than their hadronic counterparts. For example, in

$$Z^0 \rightarrow \nu_s \bar{\nu}_s \text{ with } \nu_s \rightarrow \nu \mu^+ e^- \tilde{\gamma} \text{ and } \bar{\nu}_s \rightarrow \bar{\nu} \tilde{\gamma} , \quad (11)$$

one will observe

$$e^+ e^- \rightarrow \mu^+ e^- + \text{neutrals} \quad (12)$$

with considerable missing energy and highly unbalanced p_{\perp} . Unlike in τ decays the μ^+ and the e^- will go into the same hemisphere. It is important to note that these decays are independent of the masses of the scalar quarks and gluinos. If these masses are too large, the hadronic decays could be completely suppressed without any effect on the four-body charged leptonic decays.

The angular distribution of $\nu_e \bar{\nu}_e$ events is given by eq. 9. This angular dependence peaks at an angle of 90° which maximizes p_\perp . This is very helpful in separating these events from the primary backgrounds. For example, the background of beam-gas events can be totally separated since they have $p_\perp \approx 0$. Another possible background is two-photon events where one or both energetic electrons are missed because they leave the detector through the beam pipe or a "hole" in the detector. If one is running on the Z^0 resonance as in SLC or LEP, the two-photon process is significantly reduced in its importance since it cannot proceed through the Z^0 resonance. The Z^0 resonance dominates the total cross-section and also determines the rate of scalar neutrino production. In any case, only a small number of these events will have the large p_\perp required to simulate scalar neutrino pair production. Furthermore, by omitting the small number of events where the missing momentum is pointing in the direction of a hole in the detector one can guard effectively against background from two-photon events where only one electron is missing. It should also be noted that the total phase space for such events is very small since energy-momentum conservation puts further restrictions on the missing particle. The probability of two electrons leaving the detector through a blind spot is very small for this type of event and should be sufficient in suppressing this background. Since most backgrounds of this type are continuous in the neighborhood of the "holes" one can estimate quite effectively the total contributions of such events to the background.

Our discussions with experimentalists leave us confident that our events can be totally isolated from all backgrounds even if the number of events is very small.

4. CONCLUSIONS

We have examined the production of scalar leptons via the decay of W bosons in $p\bar{p}$ scattering. It was shown that there will be substantial signals for these supersymmetric particles if they are light enough (for example, if $M_{\nu_s} = M_{e_s} \approx 30$ GeV or if $M_{e_s} \approx 40$ GeV and $M_{\nu_s} \approx 10$ GeV). The backgrounds include W decays to $e\nu$ and $\pi\nu$, semileptonic decays of heavy quarks and possible new physics. We showed that (except for unknown new physics) all backgrounds were easily handled and/or were small. With the use of experimental cuts on data, the signal for supersymmetry can be clearly separated from $W \rightarrow e\nu$ when approximately 300 $W \rightarrow e\nu$ events are accumulated.

As higher energies for e^+e^- annihilation are achieved (and especially on the Z^0 resonance), dramatic signals for scalar neutrinos may become available. These could include events with jets and a electron confined to a single hemisphere. Even more dramatic though rarer would be events in which a muon and an electron would appear together in one hemisphere and all other energy would be missing. These signals would have no backgrounds at all.

The prospect of raising substantially the limits on the masses of the supersymmetric partners of the lepton is only about two years away. With luck such particles will be discovered rather than having improved limits.

ACKNOWLEDGMENTS

We would like to acknowledge valuable discussions with Stan Brodsky, David Burke, Jonathan Dorfan, John Ellis, Fred Gilman, Bob Hollebeek, Gordon Kane, Al Odian, Michael Peskin, Dieter Schlatter, and Giora Tarnopolsky. This work was supported in part by the Department of Energy under contract number DE-

AC03-76SF00515. One of us (H.E.H.) acknowledges support by the National Science Foundation, grant PHY 8115541-02 and another of us (R.M.B.) acknowledges support by the National Science Foundation, grant PHY77-27084 (supplemented by funds from the National Aeronautics and Space Administration).

APPENDIX: Electron Spectra from Sequential W Decay

The existence of the W was first ascertained by its decay $W \rightarrow e\nu$. This was identified experimentally via $p\bar{p} \rightarrow eX$ where an isolated electron was produced at large p_T accompanied by large missing momentum (the neutrino). In this paper, we have studied whether one could find evidence for supersymmetry in $p\bar{p} \rightarrow eX$, namely in $W \rightarrow e_s\nu_s \rightarrow e\tilde{\gamma}\nu_s$ where both $\tilde{\gamma}$ and ν_s escape detection. It is important to make sure that this signal is not confused with τ decay via $W \rightarrow \tau\nu \rightarrow e\nu\nu\bar{\nu}$. To compute the relevant distributions using Monte Carlo techniques, we first compute distributions in the W rest frame and then boost the W according to its appropriate longitudinal and transverse momentum distributions given by a “QCD-improved” version of the Drell-Yan model. In the W rest frame, we have computed the angular distribution for e_s^- in $\bar{u}d \rightarrow W^- \rightarrow e_s^- \nu_s$. The e^- emerges isotropically in the rest frame of the e_s^- . This can easily be implemented in the Monte Carlo program. The case of τ is a little more involved since the τ^- is produced polarized. Thus going to the rest frame of the τ , its decay rate depends on the helicity of the τ which in turn depends on the direction it was emitted.

A second approach is to compute directly the angular and energy distribution of electrons emerging (in the W rest frame) in $\bar{u}d \rightarrow W^- \rightarrow e^- \tilde{\gamma}\nu_s$ (and similarly for the τ). These distributions were quoted in ref. 15 without derivation. Because the derivation of these results do not appear to be widely known, we present it here.

The starting point is the following formula³⁴ for the cross section of the two step process $a + b \rightarrow c + d$, $d \rightarrow 1, 2, \dots, n$:

$$\sigma = \frac{1}{2q_0 s^{1/2}} \int |T(ab \rightarrow cd)|^2 \frac{ds_d}{2\pi} d Lips(s; p_c, p_d) \quad (A.1)$$

$$\times \frac{|T(d \rightarrow 1, 2, \dots, n)|^2 d Lips(s_d; p_1, p_2, \dots, p_n)}{(m^2 - s_d)^2 + m^2 \Gamma^2}$$

where $s = (p_a + p_b)^2$, $s_d = p_d^2$, m and Γ are the mass and total width of particle d in its rest frame, and q_0 is the center of mass (CM) momentum of a and b . (It is assumed that particle d is spinless or unpolarized.) The phase space differential is defined by:

$$d Lips(s; p_1, \dots, p_n) = (2\pi)^{-3n} \prod_{i=1}^n \frac{d^3 p_i}{2E_i}. \quad (A.2)$$

In the narrow resonance approximation, the Breit-Wigner is replaced by a δ -function and the integration over s_d is immediately performed.

Let us first compute the process $\bar{u} d \rightarrow W^- \rightarrow e_s^- \nu_s \rightarrow e^- \tilde{\gamma} \nu_s$. We can write the width of $e_s^- \rightarrow e^- \tilde{\gamma}$ (neglecting final state masses) in the following Lorentz invariant manner:

$$E_d E_e \frac{d\Gamma}{d^3 p_e} = \frac{\alpha m^2}{2\pi} \delta(p_\gamma^2) \quad (A.3)$$

where E_d is the energy of the decaying e_s^- (of mass m), (E_e, \vec{p}_e) is the electron four-momentum and p_γ is the $\tilde{\gamma}$ four-momentum. Note that eq. A.3 corresponds to a total width:

$$\Gamma(e_s \rightarrow e \tilde{\gamma}) = \frac{1}{2} \alpha m. \quad (A.4)$$

Hence, from Eq. (A.1) (after using the narrow width approximation to integrate over s_d), using Eqs. (A.3) and (A.4):

$$E_e \frac{d\sigma}{d^3p_e} = \frac{1}{2\pi s} \int |T(ab \rightarrow cd)|^2 d Lips(s; p_c, p_d) \delta(p_\gamma^2) \quad (A.5)$$

where we have neglected the quark masses and $p_\gamma = p_d - p_1$. Equation (A.5) is manifestly Lorentz invariant; we may evaluate it in the CM system of the $\bar{u}d$ (the W rest frame). We then obtain:

$$d Lips(s; p_c, p_d) = \frac{q d\Omega}{16\pi^2 s^{1/2}} \quad (A.6)$$

$$|T(ab \rightarrow cd)|^2 = \frac{\frac{1}{12} g^4 s q^2 \sin^2 \theta}{(m_W^2 - s)^2 + \Gamma_W^2 m_W^2}. \quad (A.7)$$

In Eq. (A.7), q is the CM momentum of c and d , $\cos \theta = \hat{p}_b \cdot \hat{p}_d$, $g = e/\sin \theta_W$ and the factor of $1/12$ includes the Drell-Yan color factor of $1/3$ and the initial spin average factor of $1/4$.

We insert Eqs. (A.6) and (A.7) into Eq. (A.5). In the CM frame

$$p_\gamma^2 = m^2 - 2E_e(E_d - p_d \hat{p}_d \cdot \hat{p}_e) \quad (A.8)$$

where $p_d \equiv (E_d^2 - m^2)^{1/2}$ is the momentum of the decaying e_s . We must compute

$$\int d\Omega [1 - (\hat{p}_b \cdot \hat{p}_d)^2] \delta(m^2 - 2E_e(E_d - p_d \hat{p}_d \cdot \hat{p}_e)) \quad (A.9)$$

where

$$\begin{aligned} \hat{p}_b &= (0, 0, 1) \\ \hat{p}_d &= (\sin \theta \cos \phi, \sin \theta \sin \phi, \cos \theta) \\ \hat{p}_e &= (\sin \theta_e, 0, \cos \theta_e) \end{aligned} \quad (A.10)$$

Simply rotate the coordinate system so that $\Omega = (\theta', \phi')$ where:

$$\begin{aligned}\hat{p}_d \cdot \hat{p}_e &= \cos \theta' \\ \hat{p}_b \cdot \hat{p}_d &= \cos \theta' \cos \theta_e - \sin \theta' \sin \theta_e \cos \phi',\end{aligned}\tag{A.11}$$

One can immediately integrate over ϕ' and use the δ -function to integrate over $\cos \theta'$. The result for integral (A.9) is

$$\sin^2 \theta' + \sin^2 \theta_e \left(\frac{3 \cos^2 \theta' - 1}{2} \right)\tag{A.12}$$

where

$$\cos \theta' = \frac{2E_d E_e - m^2}{2E_e p_d}.\tag{A.13}$$

Hence, Eq. (A.5) finally results in

$$\frac{d\sigma}{dE_e d \cos \theta_e} = \frac{\pi \alpha^2 p_d^2 [\sin^2 \theta' + \frac{1}{2}(3 \cos^2 \theta' - 1) \sin^2 \theta_e]}{16 \sin^4 \theta_W \sqrt{s} [(m_W^2 - s)^2 + \Gamma_W^2 m_W^2]}\tag{A.14}$$

where θ' is given in Eq. (A.13). This is the desired result written down in ref. 15.

Note that the limits on E_e are $E_e^\pm = \frac{1}{2}(E_d \pm p_d)$ corresponding to $\cos \theta' = \pm 1$.

We have used to result displayed in Eq. (A.14) as a check of our Monte Carlo program. Indeed, decaying a W^- into $e^- X$ with the above distribution resulted in the same answers as the ones we obtained by starting with a $\sin^2 \theta$ distribution for the e_s^- and then decaying it (in its own rest frame) isotropically into $e^- \tilde{\gamma}$.

We now turn to the analogous computation regarding the τ : $\bar{u} d \rightarrow W^- \rightarrow \tau^- \bar{\nu}_\tau \rightarrow e^- \bar{\nu}_e \nu_\tau \bar{\nu}_\tau$. In this case, Eq. (A.1) must be modified due to the fact that τ 's produced in W -decay are polarized. Specifically, the product of matrix elements squared must be replaced by:

$$\sum_{MM'} T(ab \rightarrow cd_M) T^*(ab \rightarrow d_{M'}) T(d_M \rightarrow 1, 2, \dots, n) T(d_{M'} \rightarrow 1, 2, \dots, n).\tag{A.15}$$

However, in the context of W decay, the τ -mass is negligible hence implying that the emitted τ 's are completely left-handed. Therefore, in the helicity basis, only one term in the sum (Eq. (A.15)) survives in the $m_\tau \rightarrow 0$ limit and we may once again use Eq. (A.1). Thus, we may proceed as in the previous example. We may use the familiar ν -decay result:³⁵

$$E_d E_e \frac{d\Gamma}{d^3 p_e} = \frac{G_F^2}{3(2\pi)^4} \left\{ q^2 p \cdot (k - mS) + 2q \cdot (k - mS) q \cdot p \right\} \quad (\text{A.16})$$

where $q \equiv k - p$, E_d is the energy of the decaying τ (with four-momentum p and spin vector S) and E_e is the electron energy (with four-momentum k). In the helicity basis,

$$S = -\left(\frac{|\vec{k}|}{m_\tau}, \frac{E_d \hat{k}}{m_\tau} \right) \quad (\text{A.17})$$

corresponding to a negative helicity τ^- . Furthermore, the matrix element for $\bar{u} d \rightarrow W^- \rightarrow \tau^- \nu_\tau$ is

$$|T(ab \rightarrow cd)|^2 = \frac{\frac{1}{12} g^4 s^2 (m_\tau^2 - 2p_b \cdot k)^2}{[(m_W^2 - s)^2 + \Gamma_W^2 m_W^2]} \quad (\text{A.18})$$

where the comments made below Eq. (A.7) apply here and p_b is the four-momentum of particle b (the d -quark in this example). Hence, following the same steps as before, we obtain

$$\begin{aligned} \sigma &= \frac{g^4}{192\pi^3 m_\tau^6 s [(m_W^2 - s)^2 + m_W^2 \Gamma_W^2]} \int d\Omega_k (m_\tau^2 - 2p_b \cdot k)^2 \\ &\times [q^2 p \cdot (k - mS) + 2q \cdot (k - mS) q \cdot p] \frac{d^3 p_e}{E_e} \end{aligned} \quad (\text{A.19})$$

which is correct to leading order in m_τ . Note the m_τ^6 in the denominator above, which results from a factor $(\Gamma_\tau m_\tau)^{-1}$ (where $\Gamma_\tau = G_F^2 m_\tau^5 / 192\pi^3$) which appears when one replaces the Breit-Wigner of Eq. (A.1) by the corresponding δ -function.

To proceed, we evaluate Eq. (A.19) in the rest frame of the W^- . In that frame

$$q^2 p \cdot (k - mS) + 2q \cdot (k - mS) q \cdot p = E_e [m_\tau^2 x + \sqrt{s} (m_\tau^2 - 2E_e x) (1 - \hat{k} \cdot \hat{p})] \quad (\text{A.20})$$

where

$$x \equiv \frac{s + m^2 - (s - m^2) \hat{k} \cdot \hat{p}}{\sqrt{s}} \quad (\text{A.21})$$

and $m^2 - 2p_0 \cdot k = -\frac{1}{2}(s - m_\tau^2)(1 + \hat{p}_b \cdot \hat{k})$. The first step is to rotate the coordinate system (see Eq. (A.10) and (A.11)) so that

$$\hat{k} \cdot \hat{p} = \cos \theta \quad (\text{A.22})$$

$$\hat{p}_b \cdot \hat{k} = \cos \theta \cos \theta_e - \sin \theta \sin \theta_e \cos \phi .$$

Next, we note that the integration limits on E_e depend on $\cos \theta$. Namely, because $(k - p)^2 \geq 0$, we find $0 \leq E_e \leq m^2/x$ (where x is given by Eq. (A.21)). As a result, we must interchange the order of integration. To leading order in m_τ ,

$$\begin{aligned} \frac{d\sigma}{d\Omega_e dE_e} &= \frac{g^4 s E_e^2}{768 \pi^3 m_\tau^6 [(m_W^2 - s)^2 + m_W^2 \Gamma_W^2]} \int_0^{2\pi} d\phi \int_y^1 d \cos \theta \\ &\times (1 + \cos \theta \cos \theta_e - \sin \theta \sin \theta_e \cos \phi)^2 \\ &\times [m_\tau^2 x + \sqrt{s} (1 - \cos \theta) (m^2 - 2E_e x)] \end{aligned} \quad (\text{A.23})$$

where $y = [E_e(s + m_\tau^2) - m_\tau^2 \sqrt{s}] / [E_e(s - m_\tau^2)]$. The integration is straightforward and tedious. Indeed, the leading term in the integral is of order m_τ^6 , thus leading to a finite limit as $m_\tau \rightarrow 0$. The final results is:

$$\frac{d\sigma}{dE_e d \cos \theta_e} = \frac{\pi \alpha \sqrt{s} (1 + \cos \theta_e)^2}{36 \sin^4 \theta_W [(m_W^2 - s)^2 + \Gamma_W^2 m_W^2]} \left[1 - \left(\frac{2E_e}{\sqrt{s}} \right)^3 \right] \quad (\text{A.24})$$

where $0 \leq E_e \leq \frac{1}{2} \sqrt{s}$. This agrees with the results of ref. 15.

REFERENCES

1. P. Fayet and S. Ferrara, Phys. Rev. 32C, 249 (1977); A. Salam and J. Strathdee, Fortschritte der Phys. 26, 57 (1978); J. Wess and J. Bagger, *Supersymmetry and Supergravity* (Princeton University Press, Princeton, New Jersey, 1983).
2. D. V. Nanopoulos, A. Savoy-Navarro and Ch. Tao. eds., Proceedings of Supersymmetry vs. Experiment Workshop, CERN publication Ref. TH.3311/EP.82/63 (1982), to be published in Physics Reports. A recent summary of experimental limits can be found in ref. 5.
3. E. Witten, Nucl. Phys. B188, 513 (1981); S. Dimopoulos and H. Georgi, Nucl. Phys. B193, 150 (1981); N. Sakai, Z. Phys. C11, 153 (1981).
4. The W events have been reported in: UA1 Collaboration, G. Arinson *et al.*, Phys. Lett. 122B, 103 (1983); 129B, 273 (1983); UA2 Collaboration, G. Banner *et al.*, Phys. Lett. 122B, 476 (1983). The Z events have been reported in: UA1 Collaboration, G. Arinson *et al.*, Phys. Lett. 126B, 398 (1983); UA2 Collaboration, P. Bagnaia *et al.*, Phys. Lett. 129B, 130 (1983).
5. Recent limits on masses of supersymmetric particle were summarized by S. Yamada at the 1983 International Symposium on Lepton and Photon Interactions at High Energies. Previous published limits are: H. J. Behrend *et al.*, Phys. Lett. 114B, 287 (1982); W. Bartel *et al.*, Phys. Lett. 114B, 211 (1982); R. Brandelik *et al.*, Phys. Lett. 117B, 365 (1982); D. P. Barber *et al.*, Phys. Rev. Lett. 45, 1904 (1980); W. T. Ford *et al.*, SLAC-PUB-2986 (1982); Y. Ducros, Acta Phys. Pol. B14, 589 (1983); L. Gladney *et al.*, SLAC-PUB-3178 (1983); E. Fernandez *et al.*, SLAC-PUB-3231 (1983).

6. Models exist where R -parity is broken. The lightest supersymmetry particle would then decay into ordinary particles, e.g. $\tilde{\gamma} \rightarrow \gamma + \nu$. Such models usually lead to violation of either baryon or lepton number (as in the $\tilde{\gamma}$ decay just mentioned). For a further discussion, see L. J. Hall and M. Suzuki, preprint LBL-16150 (1983).
7. R -parity is a discrete subgroup of a more general (continuous) R -symmetry first introduced by A. Salam and J. Strathdee, Nucl. Phys. B87, 85 (1975) and P. Fayet, Nucl. Phys. B90, 104 (1975). R -parity as discussed here was first used by P. Fayet, Phys. Lett. 69B, 489 (1977).
8. One exception to these remarks concerns the gluino which can be pair produced in gluon-gluon scattering by t -channel gluino exchange. If the gluino is light, it should be copiously produced in hadron machines and might soon be observable. For a recent discussion of gluino production and further references, see: H. E. Haber and G. L. Kane, preprint UM-HE-83-18 to be published in Nucl. Phys. B.
9. H. E. Haber, R. M. Barnett and K. S. Lackner, SLAC-PUB-3224 (1983).
10. E. Cremmer, S. Ferrara, L. Girardello and A. van Proeyen, Phys. Lett. 116B, 231 (1983); Nucl. Phys. B212, 413 (1983); L. Hall, J. Lykken and S. Weinberg, Phys. Rev. D27, 2359 (1983); S. K. Soni and H. A. Weldon, Phys. Lett. 126B, 215 (1983).
11. L. Alvarez-Gaume, J. Polchinski and M. B. Wise, Nucl. Phys. B221, 495 (1983).
12. A. H. Chamseddine, R. Arnowitt and P. Nath, Phys. Rev. Lett. 49, 970 (1982); Phys. Lett. 120B, 145 (1983); Phys. Lett. 121B, 33 (1983); H. P. Nilles, Phys. Lett. 115B, 193 (1982); Nucl. Phys. B217, 366

- (1983); L. Ibanez, Phys. Lett. 118B, 73 (1982); Nucl. Phys. B218, 514 (1983); R. Barbieri, S. Ferrara and C. A. Savoy, Phys. Lett. 119B, 343 (1982); H. P. Nilles, A. Srednicki and D. Wyler, Phys. Lett. 121B, 123 (1983); E. Cremmer, P. Fayet and L. Girardello, Phys. Lett. 122B, 41 (1983); B. A. Ovrut and S. Raby, Phys. Lett. 125B, 270 (1983); J. Ellis, J. S. Hagelin, D. V. Nanopoulos and K. Tamvakis, Phys. Lett. 125B, 275 (1983); M. Claudson, L. J. Hall and I. Hinchliffe, preprint LBL-15748 (1983).
13. An extensive review including references can be found in H. E. Haber and G. L. Kane, to be published in Physics Reports. See also: I. Hinchliffe and L. Littenberg, in *Proceedings of the 1982 DPF Summer Study on Elementary Particle Physics and Future Facilities*, p. 242, edited by R. Donaldson, R. Gustafson and F. Paige (American Physical Society, New York, 1983).
 14. R. M. Barnett, K. S. Lackner and H. E. Haber, Phys. Rev. Lett. 51, 176 (1983).
 15. R. Barbieri, N. Cabibbo, L. Maiani and S. Petrarca, Phys. Lett. 127B, 458 (1983).
 16. N. Cabibbo, L. Maiani and S. Petrarca, University of Rome preprint 355 (1983).
 17. D. A. Dicus, S. Nandi and X. Tata, Phys. Lett. 129B, 445 (1983).
 18. R. Arnowitt, A. H. Chamseddine and P. Nath, Phys. Rev. Lett. 50, 232 (1983); Phys. Lett. 129B, 445 (1983); S. Weinberg, Phys. Rev. Lett. 50, 387 (1983); P. Fayet, Phys. Lett. 125B, 178 (1983); preprint LPTENS 83/35 (1983); V. Barger, R. W. Robinett, W. Y. Keung and R.J.N. Phillips, Wisconsin preprint MAD/PH/130 (1983); B. Grinstein, J. Polchinski and

- M. B. Wise, CALT-68-1038 (1983).
19. J. Ellis, J. S. Hagelin, D. V. Nanopoulos and M. Srednicki, *Phys. Lett.* **127B**, 233 (1983). D. A. Dicus, S. Nandi, W. W. Repko and X. Tata, University of Texas preprint DOE-ER-03992-521; V. Barger, R. W. Robi-
nett, W. Y. Keung and R.J.N. Phillips, Wisconsin preprint, MAD/PH/115
(1983).
 20. J.-M. Frère and G. L. Kane, *Nucl. Phys.* **B223**, 331 (1983); D. A. Dicus,
S. Nandi, W. W. Repko and X. Tata, *Phys. Rev. Lett.* **51**, 1030 (1983);
J. Ellis, J.-M. Frère, J. S. Hagelin, G. L. Kane and S. T. Petcov, SLAC-
PUB-3152 (1983).
 21. Our notation is to denote scalar leptons and quarks by adding a subscript
 s to the usual symbol. In general, there are two scalar partners f_{sL} and
 f_{sR} (partners of the left and right handed fermions), although the actual
mass eigenstates are some linear combination of the two states (depend-
ing on the unknown scalar lepton and quark matrices). There is only one
scalar neutrino ν_s (assuming the right handed neutrino is not relevant for
low energy physics). Note that in W -decay, because of the V-A interac-
tion, only the L -type scalars are produced. We will often suppress the L
subscript when no confusion can arise.
 22. F. Halzen, A. D. Martin and D. M. Scott, *Phys. Rev.* **D25**, 754 (1982).
 23. L. B. Okun and M. B. Voloshin, *Nucl. Phys.* **B120**, 461 (1977); C. Quigg,
Rev. Mod. Phys. **49**, 297 (1977); R. F. Peierls, T. L. Trueman and L. L.
Wang, *Phys. Rev.* **D16**, 1397 (1977); J. Kogut and J. Shigemitsu, *Nucl.*
Phys. **B129**, 1397 (1977); J. Ellis, M. K. Gaillard, G. Girardi and P. Sorba,
Ann. Rev. Nucl. Part. Sci. **32**, 443 (1982).

24. J. F. Owens and E. Reya, *Phys. Rev.* D17, 3003 (1978).
25. F. Paige, in *Proton-Antiproton Collider Physics*, p. 168, edited by V. Barger, D. Cline and F. Halzen (American Institute of Physics, New York, 1982).
26. D. B. Cline and C. Rubbia, *Phys. Lett.* 127B, 277 (1983). S. Gottlieb and T. Weiler, San Diego preprint (1983).
27. R. M. Barnett and H. E. Haber, in preparation.
28. R. M. Barnett, K. S. Lackner and H. E. Haber, *Phys. Lett.* 126B, 64 (1983).
29. In certain theories of supersymmetry, the dominant decay would be $\ell_s \rightarrow \ell + \tilde{G}$ where \tilde{G} is a massless spin 1/2 Goldstino (which arises when global supersymmetry is spontaneously broken). The \tilde{G} would also escape undetected so that the resulting signal would be the same as for the light photino.
30. For example, see G. Barbiellini, B. Richter and J. L. Siegrist, *Phys. Lett.* 106B, 414 (1981).
31. In this paper, we have assumed the existence of light gluinos (say, with a mass less than 5 GeV). If gluinos turn out to be substantially heavier, then, we would expect the four-body hadronic decays of the scalar neutrino to be comparable in branching ratio to the four-body leptonic decays. Under such conditions, these branching ratios would be small (less than 1%), as shown in ref. 28.
32. There are actually two fermionic states ("winos") here which we denoted in refs. 9 and 28 by ω_1 and ω_2 . In the limit that these two states are degenerate in mass with each other and with the W , one finds that ω_2

decouples from $e^+e^- \rightarrow \nu_s \bar{\nu}_s$, and only ω_1 -exchange contributes.

33. For example, in the model discussed in ref. 9 the wino masses (see ref. 32) are split due to the introduction of a Majorana mass term for the gauginos. In that case, the lighter wino is more higgsino-like and its coupling to fermions is somewhat suppressed. This effect roughly compensates the enhancement due to the virtual exchange of the wino which is now lighter than the W . The end result is that the expected $\nu_s \bar{\nu}_s$ cross section is negligibly affected. In other models where the lighter wino is more gaugino-like, the $\nu_s \bar{\nu}_s$ cross section could be substantially enhanced. By assuming that $M_{wino} = m_\omega$, we have simply been conservative in our search for supersymmetry.
34. For example, see H. M. Pilkuhn, *Relativistic Particle Physics*, (Springer-Verlag, New York, 1979).
35. For example, see D. Bailin, *Weak Interactions*, (Sussex University Press, Chatto and Windus Ltd., London, 1977).

FIGURE CAPTIONS

1. Curves of constant r are shown. $r \equiv \Gamma(W \rightarrow e_s \nu_s) / \Gamma(W \rightarrow e \nu)$ is a function of M_{ν_s} and M_{e_s} (cf. eq. 1). There is a large range of mass parameters for which the decay of the W into scalar leptons would have a significant branching ratio. Since there is virtually no limit on M_{ν_s} and the limit on M_{e_s} is about 22 GeV, even a value of $r = 0.4$ is not yet excluded.
2. The shapes of various distributions resulting from the decay of a W produced in $p\bar{p}$ collisions. We plot:
 - (a) the transverse momentum, p_e^\perp , of the observed electron;
 - (b) $p_\nu^\perp = -|\vec{p}_{\text{hadron}}^\perp + \vec{p}_e^\perp|$;
 - (c) the angle θ_{eb} of the electron with respect to the proton beam axis;
 - (d) p_m defined by eq. 6 (for $W \rightarrow e\nu$ decays p_m corresponds roughly to p_ν^\parallel);
 - (e) the transverse mass, $m_T \equiv \sqrt{p_e^\perp \cdot p_\nu^\perp}$.

The curves are normalized to equal area. In each case, the solid curves refer to $W \rightarrow e\nu$; the two other curves refer to $W \rightarrow e_s \nu_s$ where $e_s \rightarrow e\tilde{\gamma}$. The dashed curve corresponds to $M_{e_s} = 40$ GeV and $M_{\nu_s} = 10$ GeV. The dotted curve corresponds to $M_{e_s} = M_{\nu_s} = 30$ GeV.

3. The shapes of various distributions resulting from the decay of a W produced in $p\bar{p}$ collisions. For notation, see the caption to fig. 2. We have eliminated all events with $p_e^\perp > 33$ GeV, or $p_L^\perp > 35$ GeV, or $\cos \theta_{eb} > 0.7$ or $-40 < p_m < 20$ GeV. (To be complete, we display the full range of p_e^\perp despite the fact that events with $p_e^\perp > 33$ GeV have

been removed from the other graphs. Similar remarks hold for the other variables.) Although the overall normalization is arbitrary, the relative normalization of the two curves is fixed (this differs from the graphs of fig. 2).

4. The shapes of various distributions resulting from $p\bar{p} \rightarrow W + X$, $W \rightarrow \nu_\tau$, $\tau \rightarrow \nu_\tau \nu_e e$. Normalization of these curves is arbitrary. The cuts are the same as indicated in the caption of fig. 3.
5. Fraction of $e^+e^- \rightarrow \nu_s \bar{\nu}_s$ events where one of the scalar neutrinos decays into charged particles and the other one decays into invisible neutrals (solid line); and fraction of events where both scalar neutrinos decay into charged particles (dashed line). We have assumed that $M_{u_s} \approx M_{e_s}$, $M_{\tilde{wino}} = m_W$ and $M_{\tilde{\gamma}} \approx M_{\tilde{g}} \approx 0$. We choose $M_{\nu_s} = 20$ GeV; however, the curve is nearly independent of the mass scale as long as $M_{\nu_s}, M_{e_s} < m_W$. The increase of the dashed line for small $M_{e_s} (M_{u_s})$ corresponds to the production of on-shell scalar electrons (scalar u -quarks) which then decay into charged modes.
6. Simulated events of $e^+e^- \rightarrow \nu_s \bar{\nu}_s$. One of the scalar neutrinos decays into $e u \tilde{d} \tilde{g}$ and the other one decays invisibly. In these "typical events" $\sqrt{s} = 42$ GeV, and $M_{\nu_s} = 18$ GeV. Each event is shown in two views. First with the beam-pipe perpendicular to the plane of the projection and secondly with the beam-pipe going from top to bottom of the plane of projection. The beam-pipe has been marked in both views. The dotted lines correspond to the electron whereas the solid lines represent the gluino and the two quarks. The resultant hadron jets will usually be relatively narrow.

7. Simulated events of $e^+e^- \rightarrow \nu_s \bar{\nu}_s$. One of the scalar neutrinos decays into $\nu q \bar{q} \bar{g}$ and the other decays invisibly. See caption to fig. 6.
8. The ratio $R \equiv \sigma(\nu_s \bar{\nu}_s) / \sigma^{em}(\mu^+ \mu^-)$ as a function of the mass of the scalar neutrino. We have assumed that $M_{\text{wino}} = m_W$. In some models with lighter winos, the values of R could be significantly enhanced (below the Z^0 resonance). Note that this cross section will be difficult to detect unless (at least) one of the ν_s decays via charged modes.

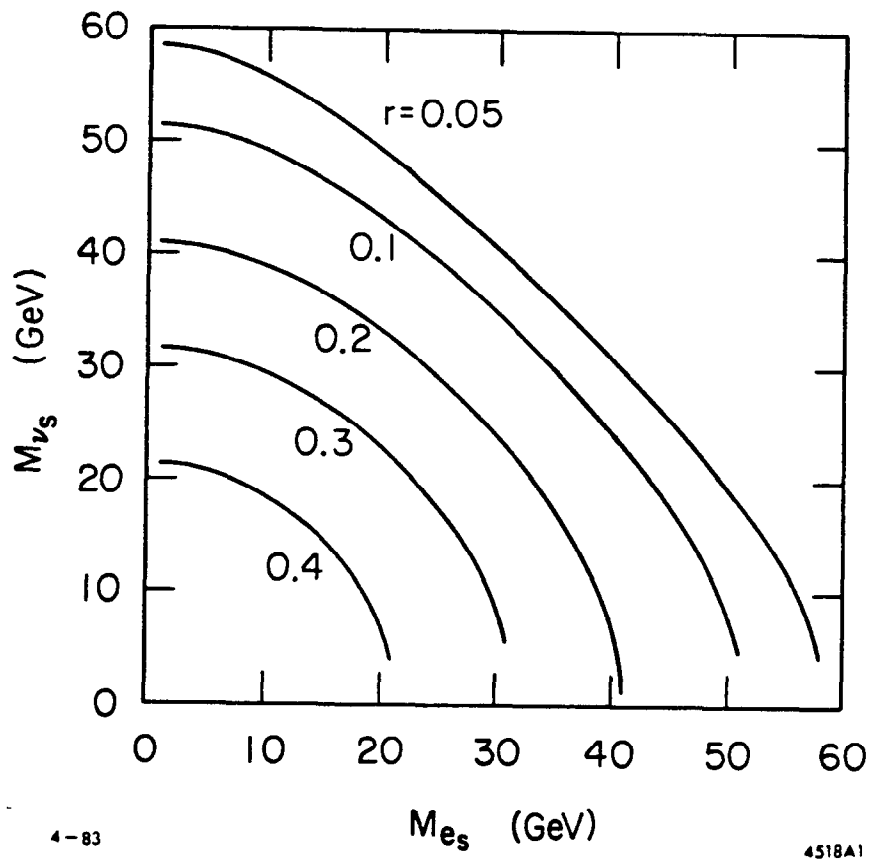


Fig. 1

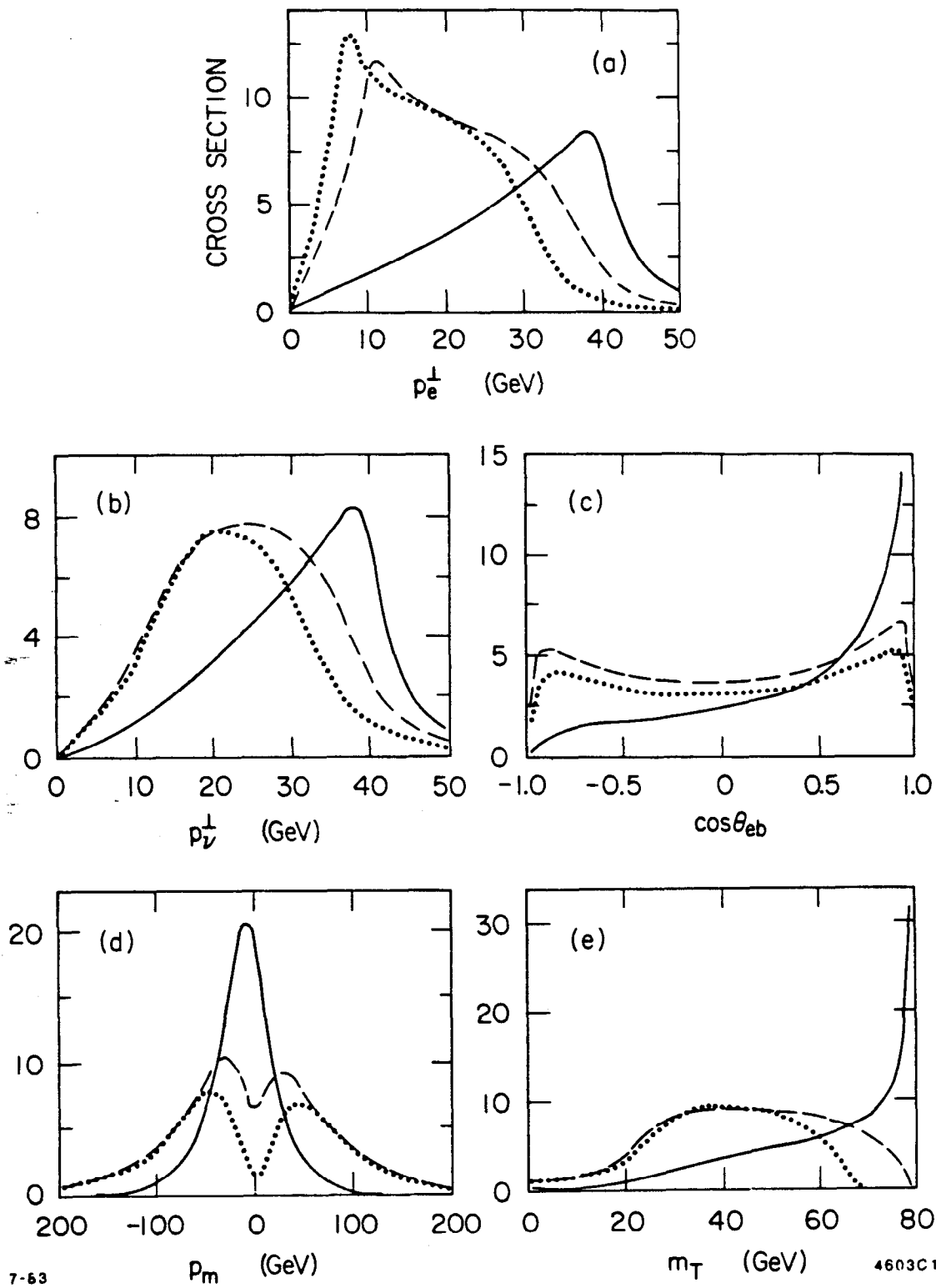


Fig. 2

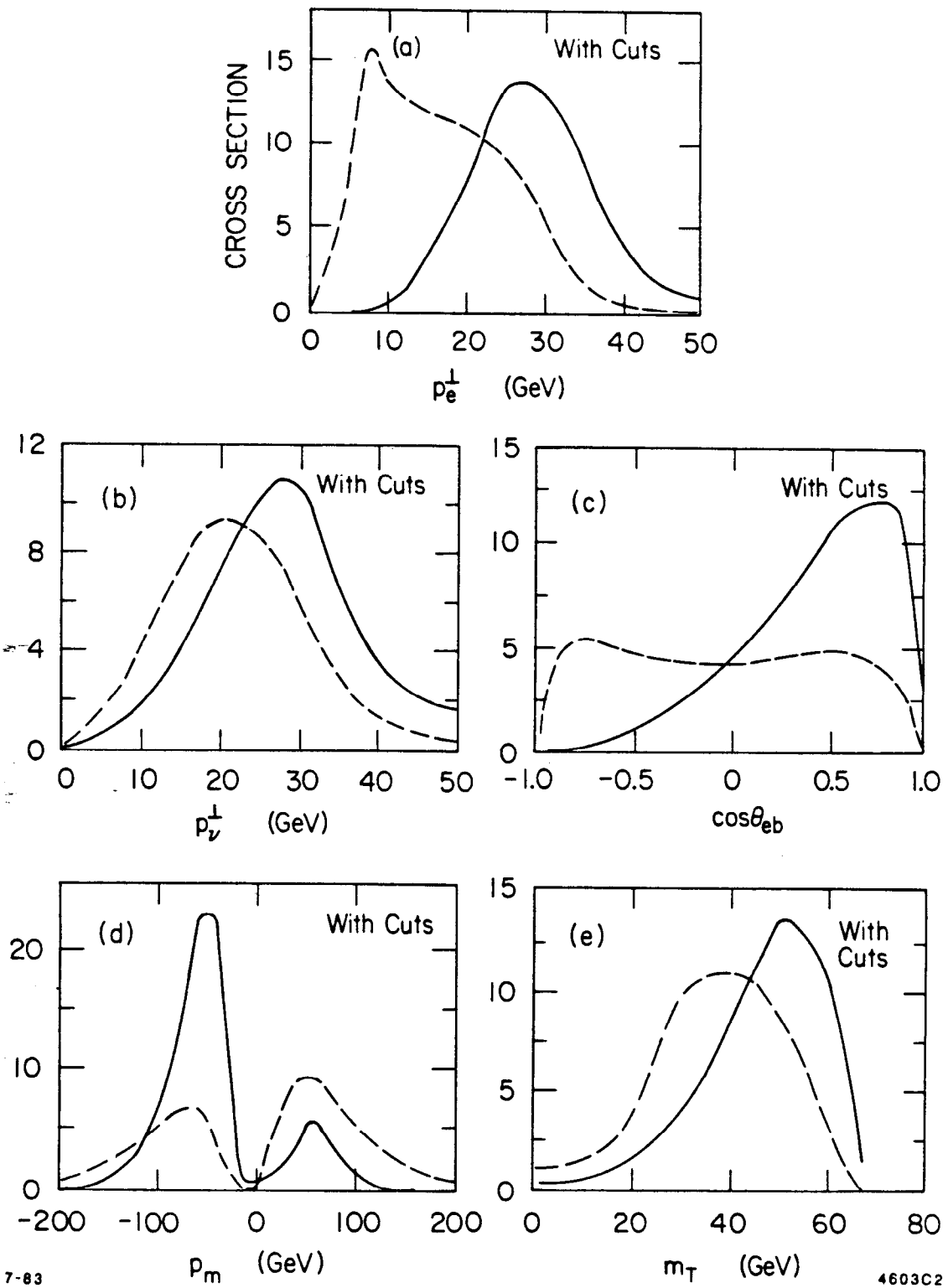


Fig. 3

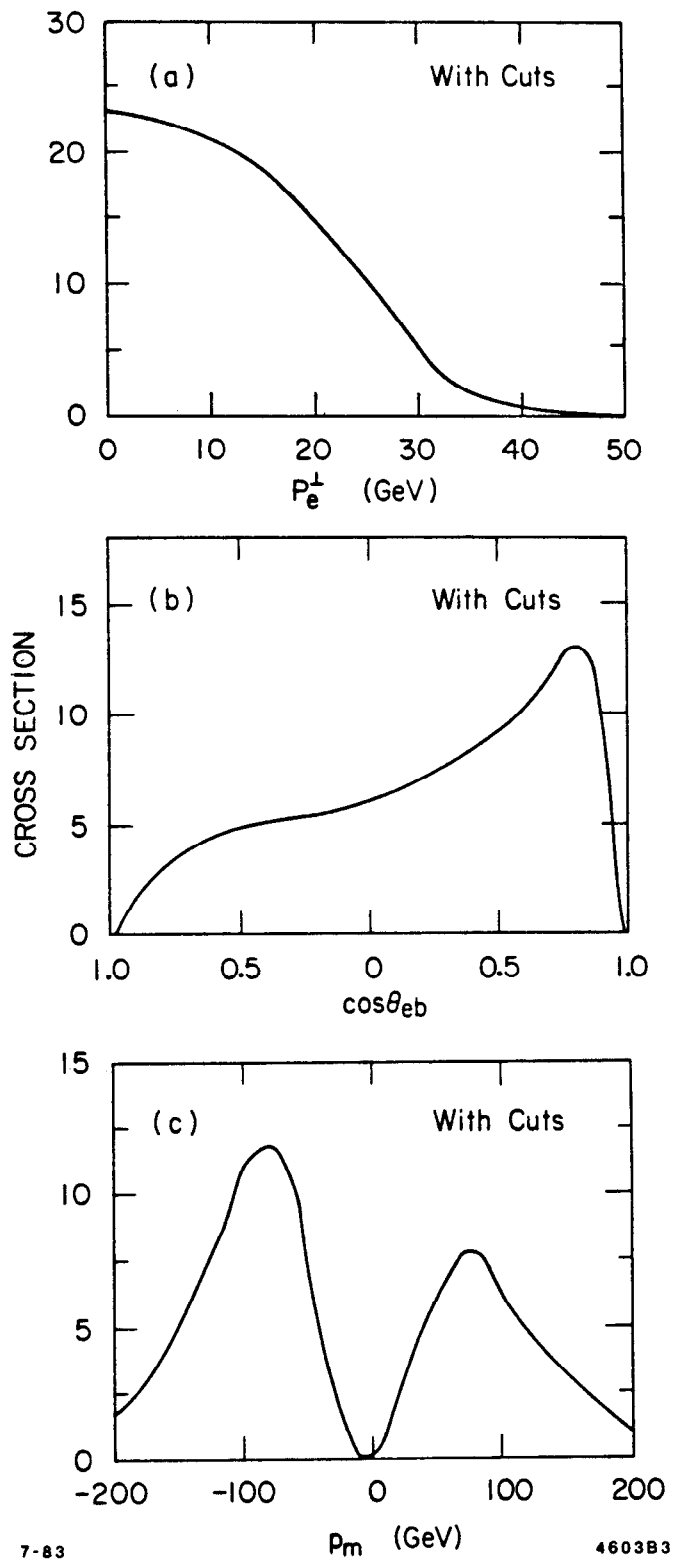


Fig. 4

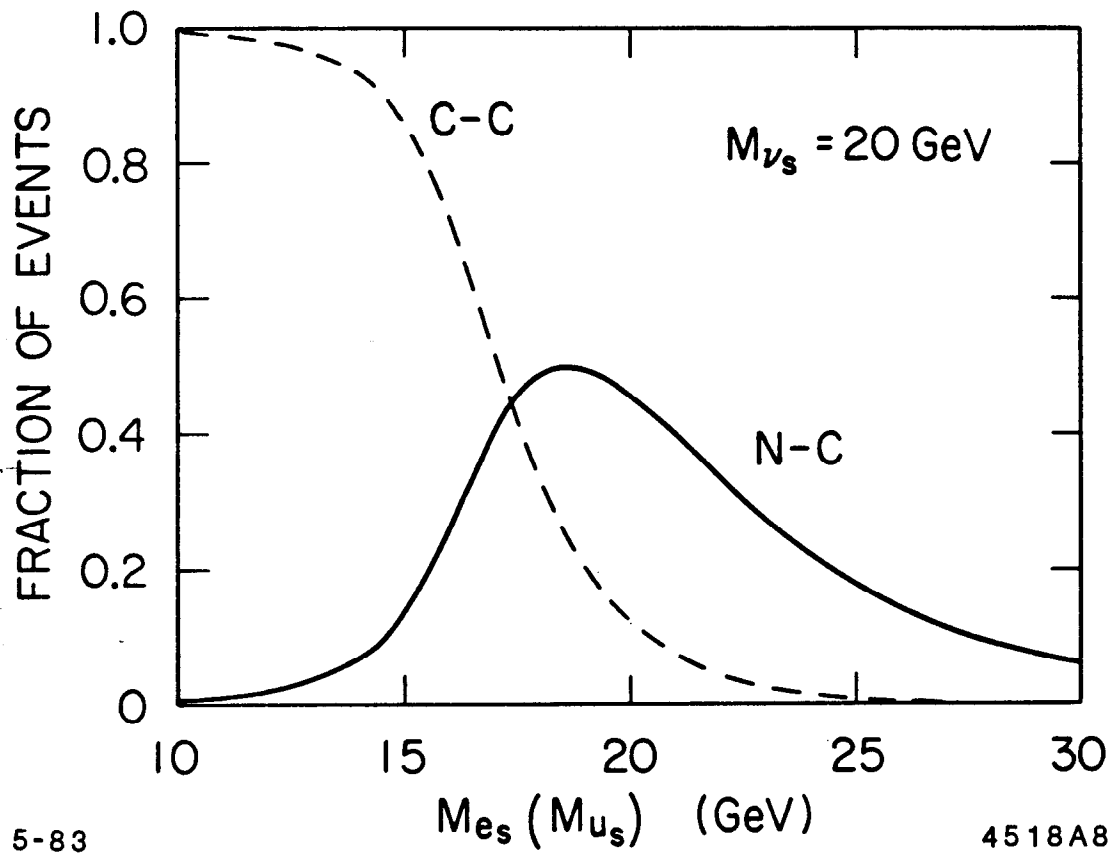
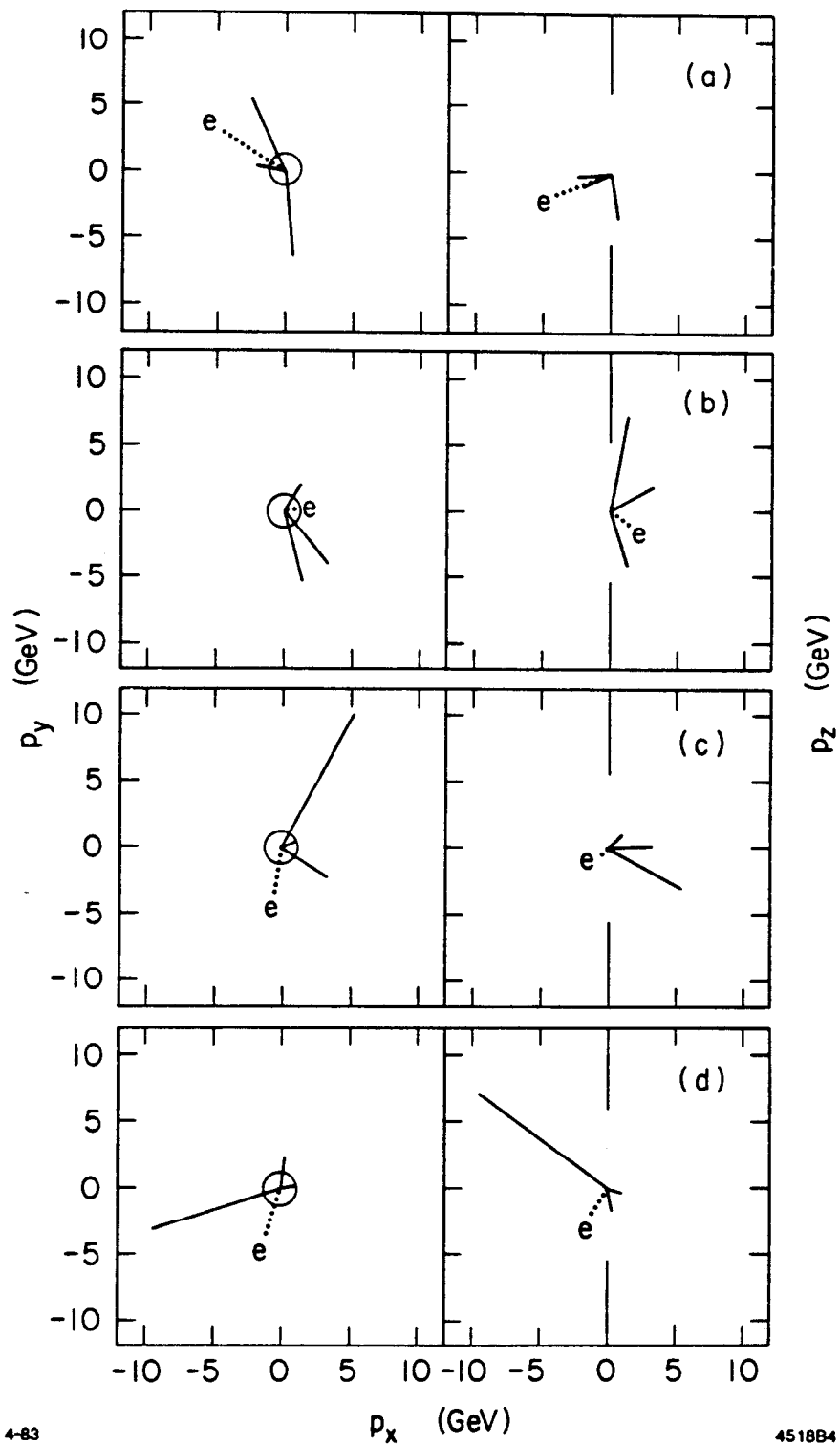


Fig. 5



4-83

4518B4

Fig. 6

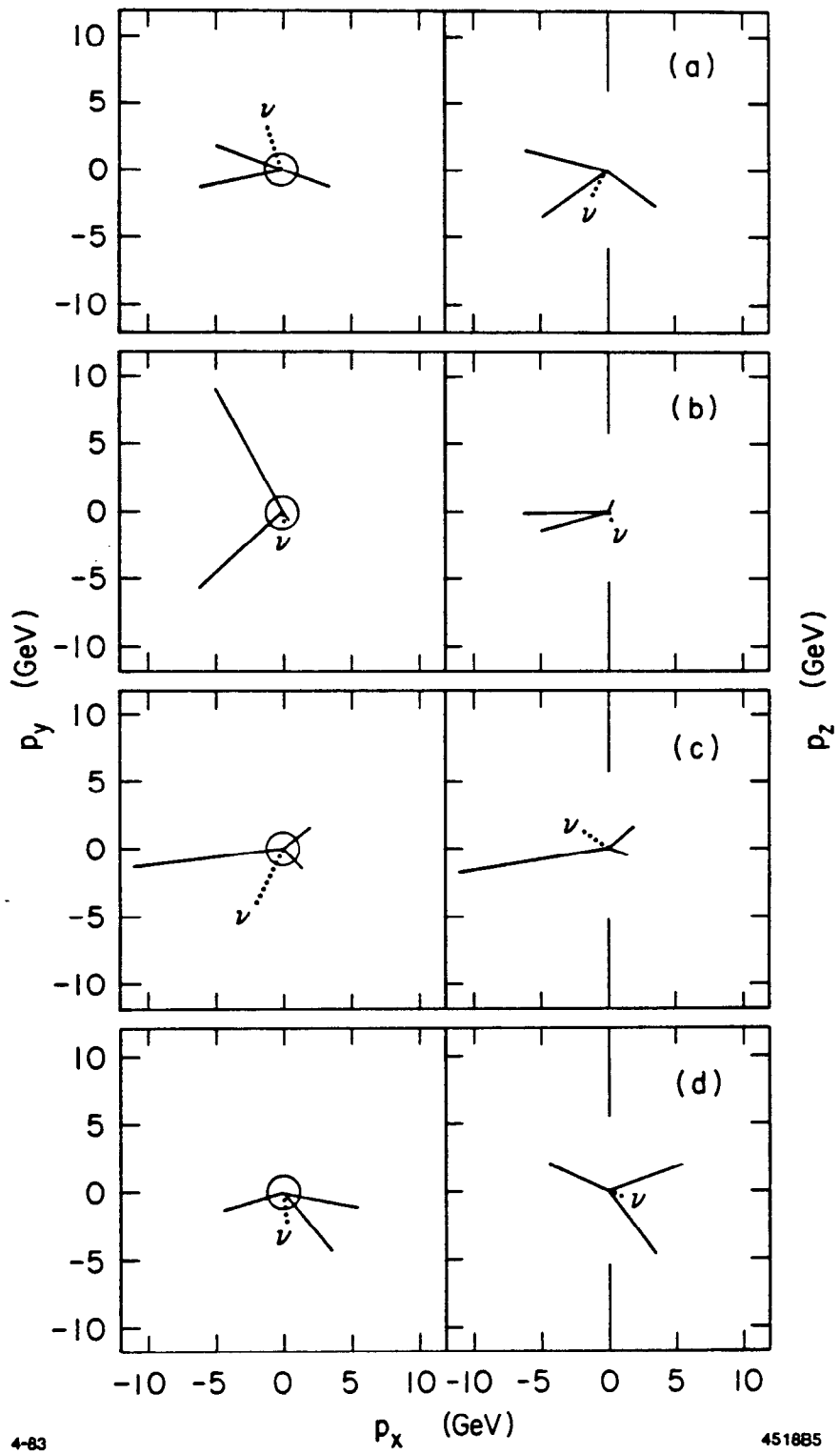


Fig. 7

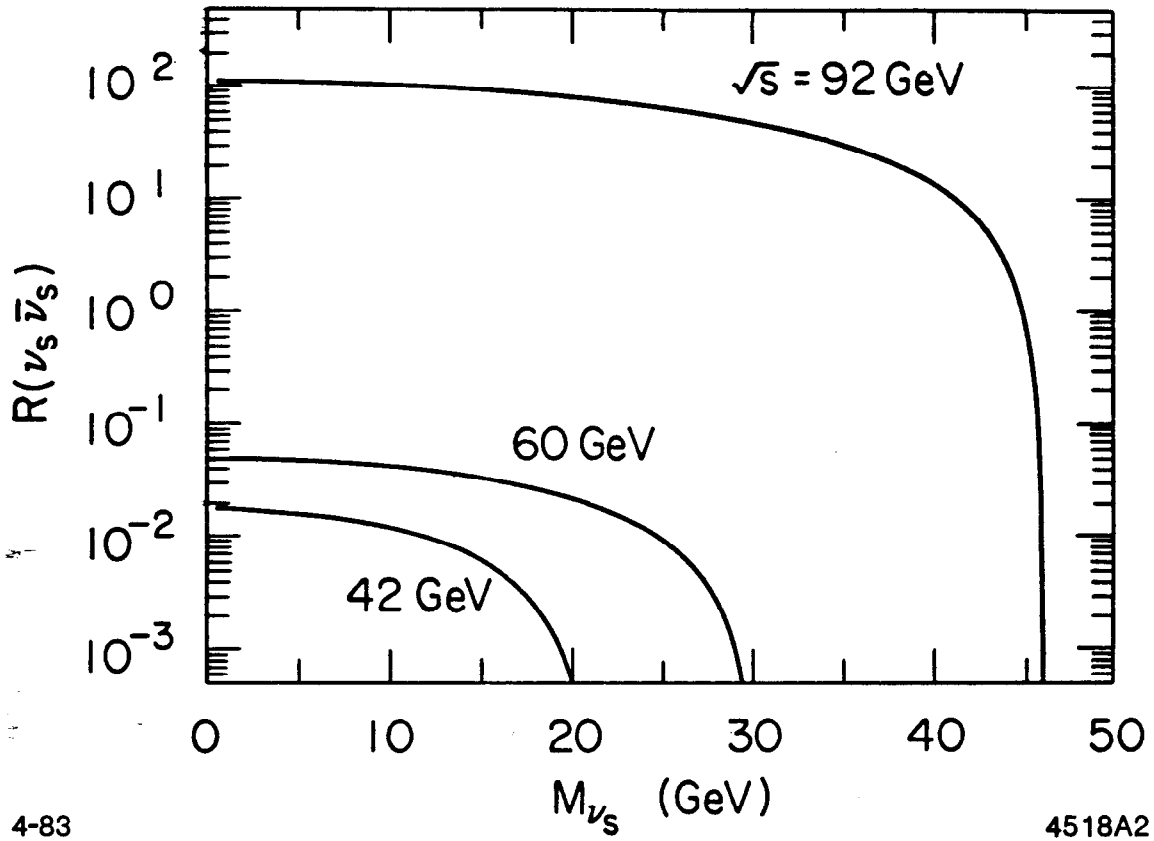


Fig. 8